

Canards and curvature: the “smallness of ε ” in slow-fast dynamics

BY MATHIEU DESROCHES[†] AND MIKE R. JEFFREY

*University of Bristol, Department of Engineering Mathematics, Queen’s Building,
University Walk, Bristol BS8 1TR, UK*

A criterion for the existence of canards in singularly perturbed dynamical systems is presented. Canards are counterintuitive solutions that evolve along both attracting and repelling branches of invariant manifolds. In two dimensions, canards result in periodic oscillations whose amplitude and period grow in a highly nonlinear way: they are slowly varying with respect to a control parameter, except for an exponentially small range of values where they grow extremely rapidly. This sudden growth, called a *canard explosion*, has been encountered in many applications ranging from chemistry to neuronal dynamics, aerospace engineering and ecology. Here we give quantitative meaning to the frequently encountered statement that the singular perturbation parameter ε , which represents a ratio between fast and slow time scales, is “small enough” for canards to exist. If limit cycles exist, then the criterion expresses the condition that ε must be small enough for there to exist a set of zero-curvature in the neighbourhood of a repelling slow manifold, where orbits can develop inflection points, and thus form the non-convex cycles observed in a canard explosion. We apply the criterion to examples in two and three dimensions, namely to supercritical and subcritical forms of the van der Pol oscillator, and a prototypical three time scale system with slow passage through a canard explosion.

Keywords: slow-fast dynamics, canard, curvature, inflection

1. Introduction

This paper uses changes of flow curvature to characterize dynamical systems of the form

$$\varepsilon \dot{x} = f(x, y, \varepsilon), \quad (1.1a)$$

$$\dot{y} = g(x, y, \varepsilon), \quad (1.1b)$$

where a singular perturbation parameter, ε , expresses the ratio between a slow time scale, t , and a fast time scale, t/ε . The variables x and y are scalars and the dot denotes differentiation with respect to time. The phrase “for small enough ε ” is often encountered in the literature discussing systems of the form (1.1) that exhibit the so-called *canard* phenomenon, and in this paper we show that this phrase can be replaced with a definite upper bound on ε , for an important class of systems.

A canard cycle is so-named because it is an orbit, solving a set of singularly perturbed ordinary differential equations, that passes between slow and fast time scales in such a way as to create a novel duck-like shape (Benoît 1981), see figure 1. In two dimensions the effect typically appears as a canard explosion: a Hopf

[†] Author for correspondence (m.desroches@bristol.ac.uk)

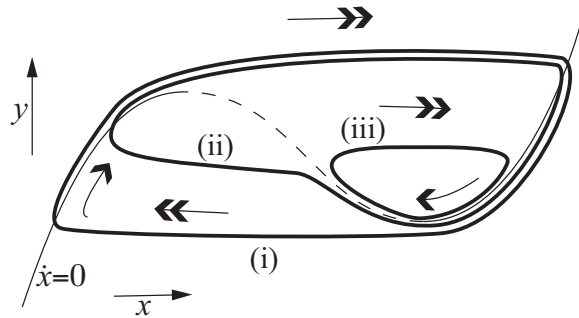


Figure 1. Canards and relaxation oscillations. Dynamics is slow (single arrows) near the curve where $\dot{x} = 0$, consisting of attracting (full curve) and repelling (dashed curve) branches. Elsewhere the dynamics is fast (double arrows) and roughly horizontal. For different parameters, this can cause a limit cycle to exist either as: (i) a relaxation oscillation, (ii) a canard with head, or (iii) a canard without head.

bifurcation generates a small near-circular limit cycle, which grows rapidly, distorting as it grows to form the characteristic canard shape (a canard “with head”, see figure 1), and eventually forming a relaxation oscillation. Small amplitude cycles enclose a convex area in state space, so that local curvature along the cycle keeps a constant sign, whereas large amplitude cycles enclose a non-convex area, so the local curvature along such a cycle undergoes a change of sign. Consequently, the canard phenomenon is characterized by the existence of a set of zero-curvature allowing the transition from (convex) small amplitude cycles to (non-convex) large amplitude cycles. An equation for this set — the *inflection curve* in planar systems — can be found using standard differential geometry of curves and surfaces. This analysis was initiated in the context of chemical models (Brøns & Bar-Eli 1994; Peng *et al.* 1991) and has been studied in a more general context recently (Ginoux & Rossetto 2006*a,b*; Ginoux 2009), though without a focus on canards. In this paper we extend the method by considering the dependence of inflection sets on the time scale ratio ε , showing that no non-convex cycles exist for ε larger than a critical value ε_0 , which can be found analytically. We use it to place an upper bound on the time scale ratio necessary for canards in two and three dimensions.

We demonstrate the inflection of canard cycles first on the van der Pol oscillator, in two different forms exhibiting supercritical and subcritical Hopf bifurcations, and then on a prototypical example of a three time scale system with two slow variables, as introduced in Krupa *et al.* (2008). This corresponds to adding a second slow time scale that stabilizes the transition through a nonhyperbolic point, resulting in slow passage through a canard explosion. We deduce from this a bound in the time scale ratio necessary for canard cycles to occur, in the parameter region where this slow passage is well-defined.

The paper is organised as follows. In section 2, we recall the basic facts about the canard phenomenon in two-dimensional slow-fast dynamical systems, using the classic example of the van der Pol oscillator. In section 3 we review results on inflection curves in two dimensions, and extend these to give a new convexity-based criterion for the existence of canard cycles. In section 4, we apply the method to a three dimensional three time scale system featuring a slow passage through a canard

explosion. Finally, in section 5 we give some conclusions and highlight directions for future research.

2. Canards in \mathbb{R}^2 : the classic van der Pol example

Consider the van der Pol equation (Van der Pol 1926) with constant forcing q

$$\varepsilon \ddot{x} + (x^2 - 1)\dot{x} + x - q = 0, \quad (2.1)$$

with $0 < \varepsilon \ll 1$, where q is a parameter. This can be expressed as a set of first-order ordinary differential equations by introducing a phase variable $u = \dot{x}$. A variant of this is to define a variable $y = \dot{x} + x^3/3 - x$, and write the system in the Liénard plane (x, y) as

$$\varepsilon \dot{x} = y - \frac{1}{3}x^3 + x, \quad (2.2a)$$

$$\dot{y} = q - x. \quad (2.2b)$$

For small ε the variable x evolves on a fast time scale t/ε , and y evolves on a slow time scale t , thus we refer to x and y respectively as fast and slow variables. The fast nullcline, where $\dot{x} = 0$, is known as the *slow curve* (or more generally *critical manifold*) of (2.2), which we label S_0 . It organises the dynamics of the system on the slow time scale, as can be seen by setting $\varepsilon = 0$. This yields a differential-algebraic system consisting of a differential equation, (2.2b), on the slow time scale, constrained by an algebraic equation, the cubic curve S_0 given by $y = \frac{1}{3}x^3 - x$. The slow curve S_0 is the phase space of this limiting problem, called the *slow subsystem* (or sometimes *reduced system*), illustrated in figure 2.

Rescaling time in (2.2) by setting $\tau = \varepsilon/t$ gives

$$x' = y - \frac{1}{3}x^3 + x, \quad (2.3a)$$

$$y' = \varepsilon(q - x), \quad (2.3b)$$

where the prime denotes differentiation with respect to τ . Taking the limit $\varepsilon = 0$ now gives a different limiting problem, where the slow variable y remains constant and can be considered as a parameter. In this way, we obtain a family of differential equations on the fast time scale parametrised by y , usually referred to as the *fast subsystem* (or sometimes *layer problem*). It is clear from equation (2.3a) that the (y -dependent) equilibria of the fast subsystem all belong to the slow curve S_0 , as shown in figure 2. These equilibria are attracting along the outermost branches S^a , and repelling along the inner branch S^r .

By combining these pictures of dynamics in the fast and slow limiting systems, (2.2) and (2.3), one obtains a first insight into the dynamics of the full system for small ε . If we take an initial condition at a distance of order 1 with respect to ε (henceforth written simply as $\mathcal{O}(1)$) away from the slow curve S_0 , the solution of the van der Pol equation first evolves on a fast time scale, almost horizontally, until it reaches an ε -neighbourhood of the attracting sheet S^a of the slow curve S_0 ; this first epoch is well captured by the horizontal fibers in the dynamics of the fast subsystem (figure 2). Once in the neighbourhood of S_0 , where $\dot{x} \approx 0$,

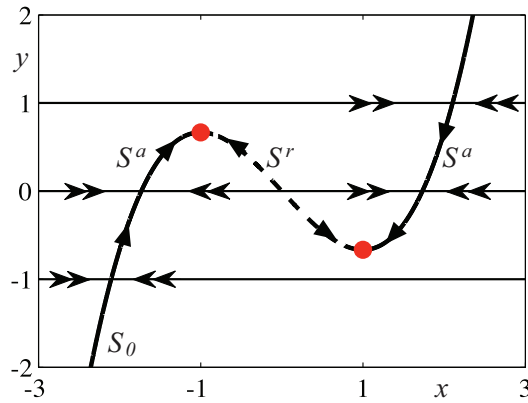


Figure 2. Fast and slow subsystems of the van der Pol equation. Single arrows indicate slow motion along the slow curve S_0 . Double arrows indicate fast motion outside S_0 , which has two attracting branches S^a and a repelling branch S^r , separated by fold points (dots) of the slow curve, which correspond to saddlenode bifurcation points of the fast subsystem.

the slow dynamics dominates and is approximated by the slow subsystem (figure 2). Hence the orbit moves slowly along S^a . This slow epoch can only end when a change of normal stability of the slow curve S^a occurs. For the van der Pol oscillator (2.2), such a change corresponds to a saddlenode bifurcation in the fast subsystem, located at folds of S_0 , which lie at $(x, y) = (-1, \frac{2}{3})$ and $(x, y) = (1, -\frac{2}{3})$, and separate the (outer) attracting branches, S^a , from the (inner) repelling branch S^r . (More generally, the normal stability of the slow curve can also change when the fast subsystem undergoes a transcritical bifurcation. Although this situation is less common in applications than the saddlenode, canard orbits can be created in this case too and they are usually referred to as *Morse-type canards* (Diener 1984).) When the slow epoch ends, the orbit re-enters the horizontal fast subsystem. As the flow makes fast jumps between passages of slow evolution along the attracting branches S^a , it is possible for a limit cycle to appear.

The limit cycle exists for parameter values $|q| < 1$, for nonzero ε . As q varies the system displays a Hopf bifurcation: for $|q| < 1$ a stable equilibrium exists on the attracting branch S^a of the slow curve, and as $|q|$ decreases through unity the equilibrium moves to the repelling branch S^r , losing stability and expelling a stable limit cycle in the process.

Phase portraits and bifurcation diagrams for different values of ε are shown in figure 3. For a moderate value of ε , the branch of limit cycles which emanates from the Hopf bifurcation at $|q| = 1$ behaves normally, in the sense that the envelope of the family of limit cycles grows as the square-root of q , consistent with the Andronov-Hopf normal form (see e.g. Kuznetsov (2004)). The bifurcation diagram is shown in figure 3(d), and a typical cycle is shown in figure 3(a). The situation for small ε is somewhat different, as shown in figures 3 (c) and (f). In figure 3 (f) we see that, close to $q = 1$, the envelope starts increasing quasi-vertically. This corresponds to an order 1 change in amplitude and period of the cycle, and it can be shown that this occurs within a band of parameter values of order $e^{-c/\varepsilon}$ for some $c > 0$. This dramatic event of an almost vertical bifurcation branch was termed a “canard

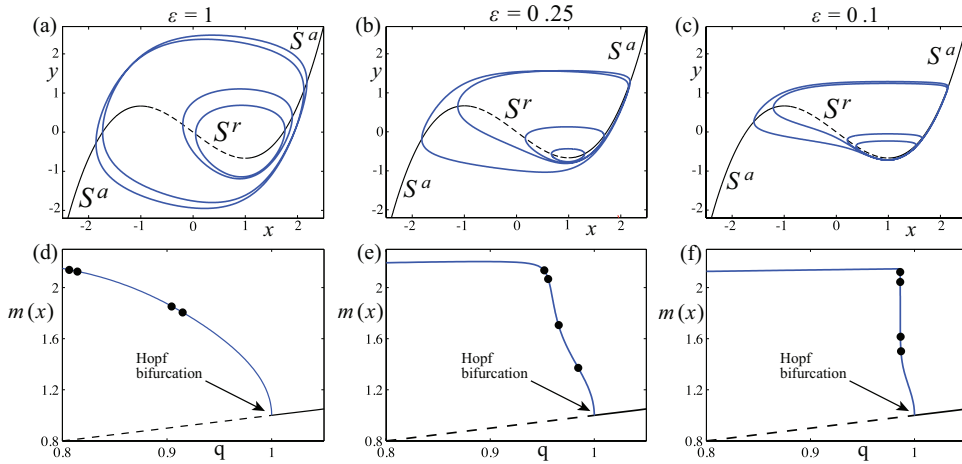


Figure 3. Comparison of four limit cycles of the van der Pol system for: (a,d) $\varepsilon = 1$, (b,e) $\varepsilon = 0.25$, (c,f) $\varepsilon = 0.1$. The limit cycles are illustrated in the (x, y) plane in (a-c), and wrap around the critical manifold $S_0 = S^a \cup S^r$. In (d-f) the bifurcation diagram is shown, where the maximum x -value, $m(x)$, along the limit cycle is plotted against the parameter q . For large ε in (a), the cycles are convex, with an amplitude in (d) that is proportional to $(q - 1)^2$ until a Hopf bifurcation at $q = 1$. For small ε in (c), large cycles are non-convex, and their amplitude in (f) jumps sharply from $m \approx 2$ to zero. In (d)-(f), dots on the bifurcation curve correspond to the four cycles shown in (a)-(c).

explosion” by Brøns (1988). Figures 3 (b) and (e) show a marginal case. Notice that, as the bifurcation in figure 3 (d)-(f) becomes more sudden, the cycle born from it in (a)-(c) becomes more distorted, forming in figure 3(c) the characteristic canard shape.

We can distinguish between two types of canard cycles, according to whether they leave the ε -neighbourhood of S^r along a fast fiber on the right as depicted in figure 2, called a *canard without head*, or on the left, called a *canard with head*. Each exist for different values of q , as depicted in figures 1 and 3. The characteristic feature of canards becomes apparent as we decrease ε , from $\varepsilon = 1$ in figure 3(a) to $\varepsilon = 0.1$ in figure 3(c). In figure 3(a), a moderate value of ε gives limit cycles that are convex for any q , and would not be called canards. In figure 3(c), ε is small enough that smaller limit cycles are convex (canards without) while larger cycles are non-convex (canards with head). Both are necessary to constitute a canard explosion. In the next section we will turn this distinction into a precise criterion for the existence of non-convex cycles, and hence of canards.

Before proceeding, for completeness we remark that the canard cycles’ counter-intuitive ability to evolve along the repelling branch, S^r , can be understood from the viewpoint of invariant manifolds. The slow curve S_0 is a set of equilibria of the fast subsystem and, as such, it is an invariant manifold. However, it is associated with the singular limit $\varepsilon = 0$. The question of the persistence of invariant manifolds was addressed by Hirsh *et al.* (1977) and, more specifically in the context of singularly perturbed dynamical systems, by Fenichel (1972, 1979). In particular, Fenichel proved that compact normally hyperbolic subsets of an invariant manifold, such as S_0 in the present case, persist as locally invariant manifolds (generally non-unique) for every small enough $\varepsilon > 0$. Furthermore, these locally invariant manifolds

are smooth ε -perturbations of the unperturbed object. In planar systems, normal hyperbolicity is generically lost at isolated fold points, which separate attracting sheets from repelling ones. Therefore, in the case of a cubic one-dimensional invariant manifold, one can apply Fenichel theory everywhere but at the two fold points. This guarantees the existence of attracting and repelling manifolds of slow motion, called *slow manifolds*, for every sufficiently small ε . Their behaviour is predicted by Fenichel theory up to the fold points, however they can always be extended past the folds by following the flow. Analytical techniques, such as parameter blow-up, can then be used to prove intersections of slow attracting and repelling manifolds, and hence the existence of canard solutions, past non-hyperbolic points; for more details, see Krupa & Szmolyan (2001) and Wechselberger (2005). A method to study such points using nonsmooth approximations, obtained by “pinching” state space around the fold, has also been discussed recently by Desroches & Jeffrey (2011), and extends the original studies of canards in terms of nonstandard analysis by Benoît et al 1981.

3. An inflection criterion for the existence of canards

Evidently, the appearance of canard cycles — convex when they are without head, non-convex when they are with head — is intimately related to the flow curvature. In two dimensions this can be understood by studying inflection points of the canard cycles. We remark in a related work (Desroches & Jeffrey 2011), where extreme changes of curvature and canards are described in the language of piecewise-smooth systems, that torsion comes into effect in three dimensions, for instance in the appearance of spiking oscillations in the Hindmarsh-Rose model (Hindmarsh & Rose 1984). The use of such higher-curvatures to infer the locations of slow manifolds is well studied by Ginoux (2009), and their relation to canards is the subject of ongoing study.

In this section we present a simple result that uses flow curvature to give a criterion to establish when canard cycles are possible. We can paraphrase this criterion as:

A singularly perturbed system may contain canard cycles only if a locus of zero-curvature exists in the neighbourhood of the repelling sheet S^r of the critical manifold $S_0 = S^a \cup S^r$.

We first derive this as a rigorous condition in the familiar context of the planar van der Pol oscillator, before applying it to general Liénard-type systems, and finally (in section 4) to an example in three dimensions.

(a) Convexity of canard cycles in the van der Pol system

Look again at the canard cycles of the van der Pol oscillator in figure 3(c). Hitherto we have distinguished canard types by whether, after traveling along the repelling branch S^r of the critical manifold, they curve away from S^r to form a small cycle (canard without head) or a large cycle (canard with head). An alternative is to express this difference in terms of local curvature along the canard cycles, specifically whether their curvature changes near the repelling branch S^r of the critical manifold, as depicted in figure 4. When the canard develops a head, its

orbit in the Liénard plane undergoes a change in the sign of its curvature, which causes the canard with head to enclose a non-convex region of the plane. This non-convexity arises from competition between the slow time scale, which pulls the cycle along S^r , and the fast time scale, which pulls the cycle away from S^r . The idea of using this to quantify time scale separation was introduced by Peng *et al.* (1991), in the context of two-dimensional singularly perturbed chemical systems exhibiting a canard explosion. Brøns and Bar-Eli (1994) developed the idea further and compared it with other techniques used to characterise canard explosions (e.g. invariant manifolds, asymptotics). In particular, they showed that the asymptotic expansion in ε of the repelling slow manifolds — whose existence are guaranteed close to S^r by Fenichel theory — coincides with the inflection curves to first order in ε . Here we extend this to form an explicit criterion for the existence of canards.

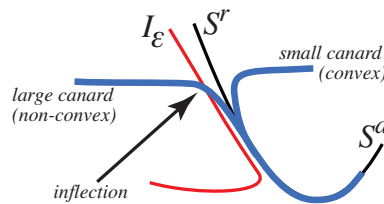


Figure 4. Curvature of a large canard cycle (with head) and small canard cycle (without head) near the repelling branch S^r of the critical manifold. A large canard cycle is characterised by the presence of an inflection point that makes it non-convex. Hence it crosses the inflection line I_ε whereas the small canard does not.

The radius of curvature $1/\kappa$ of a planar curve $y = y(x)$ is given (see e.g. Bruce & Giblin (1992)) by the formula

$$\kappa(x) = \frac{y''(x)}{(1 + y'(x)^2)^{3/2}}. \quad (3.1)$$

Consider the planar singularly perturbed system (1.1). Its trajectories can be expressed by eliminating time from (1.1) by calculating $dy/dx = \varepsilon g(x, y, \varepsilon)/f(x, y, \varepsilon)$, or, more conveniently,

$$f(x, y, \varepsilon) \frac{dy}{dx} = \varepsilon g(x, y, \varepsilon). \quad (3.2)$$

Differentiating with respect to x gives

$$\frac{dy}{dx} \frac{d}{dx} f(x, y, \varepsilon) + \frac{d^2 y}{dx^2} f(x, y, \varepsilon) = \varepsilon \frac{d}{dx} g(x, y, \varepsilon). \quad (3.3)$$

The locus of zero curvature of the vector field is where $\kappa(x) = 0$. This implies $y''(x) = 0$ by (3.1), hence (3.3) becomes

$$g(x, y, \varepsilon) \frac{d}{dx} f(x, y, \varepsilon) = f(x, y, \varepsilon) \frac{d}{dx} g(x, y, \varepsilon). \quad (3.4)$$

Because a canard with head has a change in the sign of its local curvature near the repelling slow manifold, it should cross the set $\kappa(x) = 0$. As it does so it develops

an inflection point, so the curves $\kappa(x) = 0$ are sometimes called inflection curves. If no inflection curves exist then all cycles in the plane must be convex, from which we infer that there is no significant separation of time scales, and hence there are no canards.

(b) *Inflection curves in Liénard-type systems*

Liénard systems are second-order differential equations of the form $\ddot{x} + F(x)\dot{x} - g(x) = 0$ where F and g are even and odd functions of x respectively. They play an important role in many applications (models of electronic circuits, neuron dynamics, mechanical systems *etc.*) and possess strong properties regarding existence of limit cycles. The van der Pol oscillator is an example of a Liénard system with $F(x) = x^2 - 1$. A disparity of time scales between the x and \dot{x} dynamics arises if instead the Liénard equations take the form

$$\varepsilon\ddot{x} + F(x)\dot{x} - g(x) = 0 \quad (3.5)$$

for a small parameter ε , where the function F is assumed to be well defined and at least Lipschitz continuous on \mathbb{R} . Let f be a function on the real line such that $f'(x) = F(x)$. Then, by setting $y = \varepsilon\dot{x} + f(x)$, we can rewrite (3.5) as a system of first-order differential equations,

$$\varepsilon\dot{x} = y - f(x), \quad (3.6a)$$

$$\dot{y} = g(x). \quad (3.6b)$$

Trajectories of this system satisfy

$$(y - f(x))\frac{dy}{dx} = \varepsilon g(x). \quad (3.7)$$

Differentiating (3.7) with respect to x , and setting $d^2y/dx^2 = 0$ to find an inflection curve, yields

$$\left(\frac{dy}{dx}\right)^2 - f'(x)\frac{dy}{dx} - \varepsilon g'(x) = 0. \quad (3.8)$$

Substituting in dy/dx from (3.7), and defining a new variable $h = y - f(x)$, we find that the inflection curve of the Liénard system (3.6) is given by

$$g'(x)h^2 + f'(x)g(x)h - \varepsilon g(x)^2 = 0. \quad (3.9)$$

This quadratic equation depending on x has, for fixed ε , two solution branches $h = h_{\pm}(x)$, which in turn give two branches $y = y_{\pm}(x)$ given by

$$y_{\pm}(x) = f(x) - \frac{g(x)}{2g'(x)} \left[f'(x) \pm \sqrt{f'(x)^2 + 4\varepsilon g'(x)} \right]. \quad (3.10)$$

The inflection curve exists only if the solutions of (3.10) are real, hence

$$y_{\pm}(x) \in \mathbb{R} \Rightarrow (f'(x))^2 + 4\varepsilon g'(x) > 0. \quad (3.11)$$

Notice that this condition depends on ε . Clearly the condition is satisfied trivially if $g'(x) > 0$ for all x .

In the case of the van der Pol oscillator with $f(x) = x^3/3 - x$ and $g(x) = q - x$, (3.11) implies $(x^2 - 1)^2 - (2\sqrt{\varepsilon})^2 > 0$. From this we find that for an inflection curve to exist we must have

$$\text{either} \quad f'(x) > +2\sqrt{\varepsilon} \iff x^2 > 1 + 2\sqrt{\varepsilon}, \quad (3.12a)$$

$$\text{or} \quad f'(x) < -2\sqrt{\varepsilon} \iff x^2 < 1 - 2\sqrt{\varepsilon}. \quad (3.12b)$$

Condition (3.12a) always has real solutions, but gives inflection curves in the regions $|x| > \sqrt{1 + 2\sqrt{\varepsilon}}$. These lie outside the folds of the critical manifold $y = f(x)$ in the van der Pol system (at $x = \pm 1$), and therefore not in the neighbourhood of the repelling critical manifold S^r . We are therefore interested only in condition (3.12b), which gives inflection curves in the region $|x| < \sqrt{1 - 2\sqrt{\varepsilon}}$, which does contain the repelling slow manifold, and these have real solutions only if $1 - 2\sqrt{\varepsilon} > 0$. Thus we expect canards consisting of both large non-convex and small convex cycles in the van der Pol oscillator, only if

$$\varepsilon < \varepsilon_0 := \frac{1}{4}. \quad (3.13)$$

We illustrate this criterion in figure 5, showing the inflection curves for the different values of ε illustrated earlier in figure 3. For $\varepsilon > \frac{1}{4}$ in figure 5(a), limit cycles appear almost circular, and the inflection curve exists only for $|x| > 1$. For the marginal case $\varepsilon = \frac{1}{4}$ in figure 5(b), the inflection curves still exist only for $|x| > 1$ but are noticeably deformed, and the cycle is developing an inflection. For $\varepsilon < \frac{1}{4}$ in figure 5(c), a closed inflection curve has appeared in the region $|x| < 1$ close to S^r , the cycle becomes non-convex where it crosses the curve, and is recognisably a canard. Thus the inflection condition $\varepsilon < \frac{1}{4}$ clearly captures the characteristic canard shape, whereas the convex cycles for $\varepsilon > \frac{1}{4}$ more closely resemble moderate distortions of circular cycles. The corresponding bifurcation diagrams, shown in figure 3(d)-(f), illustrate the correlation between these visual considerations of convexity, and the steepness of the bifurcation curve. Of course these are qualitative observations, but the requirement that an inflection curve exists in the neighbourhood of the repelling slow manifold solidifies them into a quantitative condition.

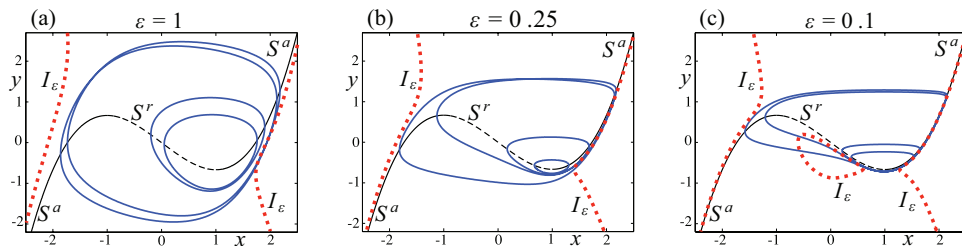


Figure 5. Comparison of four limit cycles of the van der Pol system for: (a) $\varepsilon = 1$, (b) $\varepsilon = \varepsilon_0 = 0.25$, (c) $\varepsilon = 0.1$. These orbits corresponds to those shown in figure 3 (a-c), with the inflection curves I_ε now also shown (dotted). Notice that I_ε has a branch in the neighbourhood of S^r only in (c), when ε is small enough, and (b) is the marginal case where this branch vanishes.

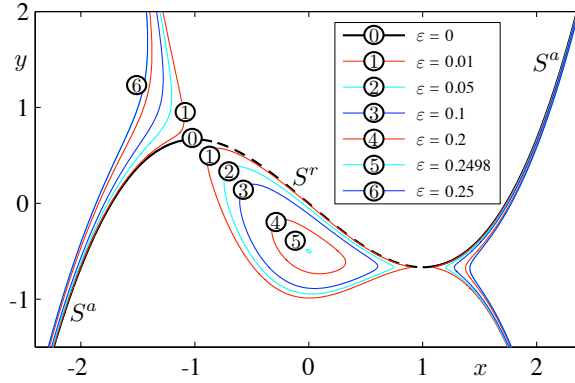


Figure 6. Comparison of the zero-curvature curves for the van der Pol system for five different values of ε ranging from 0.01 to 0.25, respectively, as indicated in the legend.

The inflection curves for several different values of ε are plotted in figure 6. For the singular value $\varepsilon = 0$ the inflection curve coincides with the critical manifold S_0 . For finite ε it splits into three branches: two open curves in the regions $|x| > 1$, and a closed loop in the neighbourhood $|x| < 1$ of the repelling critical manifold S^r . As ε increases this closed loop shrinks, until it vanishes at $\varepsilon = \frac{1}{4}$.

We therefore propose this upper bound in ε , which is obviously system dependent, as a test for the existence of a well-defined canard explosion. If the parameter ε is too large, then the sharp change of local curvature, which is one of the most prominent characteristics of the planar canard phenomenon, disappears.

(c) *Convexity of canard cycles in the FitzHugh-Nagumo equations*

Let us now look at the FitzHugh-Nagumo equations (FitzHugh 1961), which can be expressed in an abstract form as a subcritical case of the van der Pol oscillator. The equations read

$$\varepsilon \dot{x} = y - \frac{1}{3}x^3 + rx, \quad (3.14a)$$

$$\dot{y} = q - px - y. \quad (3.14b)$$

Let us fix $r > 0$ so that the critical manifold S_0 , which is now the cubic curve

$$\{(x, y) \in \mathbb{R}^2; y = f(x) = \frac{1}{3}x^3 - rx\},$$

has two fold points (where $f'(x) = 0$), at $(x, y) = \pm\sqrt{r}(1, -\frac{2}{3})$. Let us also fix $p > r$ and consider q as a bifurcation parameter. In this case the determinant $\Delta = (3q/2)^2 + (p-r)^3$ of the cubic equation satisfied at a zero of (3.14), is strictly positive for any real number q . The system (3.14) then has a unique equilibrium of focus type, and changes stability at a subcritical Hopf bifurcation (where $f'(x) = -\varepsilon$) with the emergence of an unstable limit cycle. First let us express (3.14) in the more general form

$$\varepsilon \dot{x} = y - f(x), \quad (3.15a)$$

$$\dot{y} = g(x) - y, \quad (3.15b)$$

where f and g are a real cubic function and a real affine function, respectively. Following the steps described in the two previous sections, one can easily calculate the inflection equation associated with (3.15), given by (omitting arguments)

$$(f' - g')h^2 + (f - g)(f' + \varepsilon)h + \varepsilon(f - g)^2 = 0, \quad (3.16)$$

with $h(x, y) = y - f(x)$. The solution branches $y = y_{\pm}(x)$ of the inflection equation (3.16) are then given by

$$y_{\pm} = f + \frac{(g - f)(f' + \varepsilon) \pm |g - f|\sqrt{(f' - \varepsilon)^2 + 4\varepsilon g'}}{2(f' - g')}. \quad (3.17)$$

We then investigate the presence of real solutions to the inflection equation (3.16) close to the repelling part S^r of the critical manifold S_0 when the small parameter ε is increased. From (3.17), this requires

$$(f'(x) - \varepsilon)^2 + 4\varepsilon g'(x) > 0$$

for x close to S^r . Taking f and g as in the FitzHugh-Nagumo system (3.14), this condition implies that, for an inflection curve to exist near S^r , we must have $(x^2 - (r + \varepsilon))^2 - 4\varepsilon p > 0$ with $|x| < \sqrt{r}$. This gives

$$\text{either} \quad x^2 > r + \varepsilon + 2\sqrt{\varepsilon p}, \quad (3.18a)$$

$$\text{or} \quad x^2 < r + \varepsilon - 2\sqrt{\varepsilon p}. \quad (3.18b)$$

Clearly, condition (3.18a) is incompatible with $|x| < \sqrt{r}$, hence, we focus on the second condition. Since $\varepsilon > 0$, we have

$$r + \varepsilon - 2\sqrt{\varepsilon p} > 0 \iff \sqrt{\varepsilon} \in (0, \sqrt{p} - \rho_-) \cup (\sqrt{p} + \rho_+, +\infty), \quad (3.19a)$$

$$r + \varepsilon - 2\sqrt{\varepsilon p} < 0 \iff \sqrt{\varepsilon} \in (\sqrt{p} - \rho_-, \sqrt{p} + \rho_+). \quad (3.19b)$$

where $\rho_{\pm} = \sqrt{p \pm r}$. We know that the inflection lines do exist for $\varepsilon = 0$, therefore the range of ε values must include 0, hence we can exclude both (3.19b) and the unbounded interval in (3.19a). For (3.14) with $p > r > 0$, we are left with the following condition on ε for the existence of canards:

$$0 < \varepsilon < \varepsilon_0 := (\sqrt{p} - \sqrt{p - r})^2. \quad (3.20)$$

To illustrate this let us take $r = 1$ and $p = 1.5$, then the canard criterion becomes $\varepsilon < \varepsilon_0 = (\sqrt{1.5} - \sqrt{0.5})^2 \approx 0.2679$. In figure 7 we plot limit cycles of the FitzHugh-Nagumo system (3.14), clearly showing the transition from convex to non-convex cycles as this criterion is violated, and as the inflection curve close to S^r vanishes, hence faithfully capturing the existence of canards.

4. The inflection curve method in \mathbb{R}^3

(a) Three time scale systems: slow passage through a canard explosion

The dynamics of singularly perturbed systems with canards in \mathbb{R}^3 can be much richer than the phenomena considered above, motivating the search for simple criteria to identify them. In this section we consider systems with two slow variables and

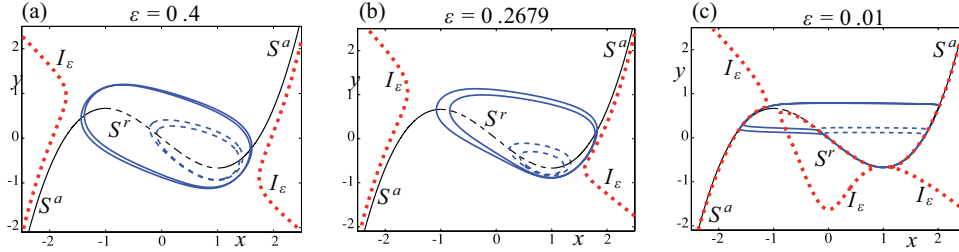


Figure 7. Comparison of four limit cycles of the FitzHugh-Nagumo system, for: (a) $\varepsilon = 0.4$, (b) $\varepsilon = \varepsilon_0 = 0.2679$, (c) $\varepsilon = 0.01$. Two stable and two unstable cycles are shown (full and dashed respectively). In (a) all cycles are convex and there is no inflection curve I_ε (dotted) near the unstable slow manifold S^r . In (c), large cycles are clearly non-convex, and I_ε has a branch close to S^r . (b) shows the marginal case, at which the inner loop of I_ε vanishes. These apply to the system (3.14) for $r = 1$ and $p = 1.5$.

one fast. These can exhibit small oscillations on the slow time scale alternating with one or several large excursions on the fast time scale. These complex oscillations are often called “mixed-mode oscillations (MMOs)”, and canards have been shown to play a key role in their organisation (Wechselberger 2005; Popovic 2008; Desroches, Guckenheimer *et al.* 2011). In most situations studied to date, these canards are due, similar to those considered above, to the presence of non-hyperbolicity associated with folds of a critical manifold, in particular so-called *folded singularities*.

Here we focus on a particular system that exhibits the classical canard explosion over a planar two-dimensional subsystem and, by means of a third even slower variable, contains a weak return through a region of small oscillations near a fold. This is referred to as a slow passage through a canard explosion. Such a system was analysed in Krupa *et al.* (2008), where the following prototypical model was introduced:

$$\varepsilon \dot{x} = f_2 x^2 + f_3 x^3 - y, \quad (4.1a)$$

$$\dot{y} = x - z, \quad (4.1b)$$

$$\dot{z} = \varepsilon(\mu - g_1 y). \quad (4.1c)$$

A mixed-mode oscillation in this system is shown in figure 8, along with the critical manifold S_0 where $\dot{x} = 0$. The system possesses three explicit time scales: fast (t/ε), slow (t), and super-slow (εt). We can gain some intuition into its dynamics by considering the planar fast subsystem (4.1a)-(4.1b) in the fast time $\tau = t/\varepsilon$, and treating the slowly varying z as a parameter. This system itself is singularly perturbed. The fast subsystem has a cubic critical manifold $y = f_2 x^2 + f_3 x^3$, making it similar to the van der Pol oscillator considered in section 3. As z varies this displays a canard explosion, and in the full system z facilitates a (super-)slow drift through the family of canard cycles, in conjunction with a weak return mechanism which re-injects orbits from post-explosion z values to pre-explosion z values.

This regime of dynamic canard explosion occurs only when $\mu + g_1$ is of $\mathfrak{o}(1)$ relative to ε , i.e. small. Two additional cases that exhibit interesting oscillatory solutions arise when both μ and g_1 are of $\mathfrak{O}(1)$, or when μ is small and g_1 is of $\mathfrak{O}(1)$. In the first case, periodic mixed-mode oscillations have a simple pattern of alternation between small and large amplitude oscillations, organised by canards at

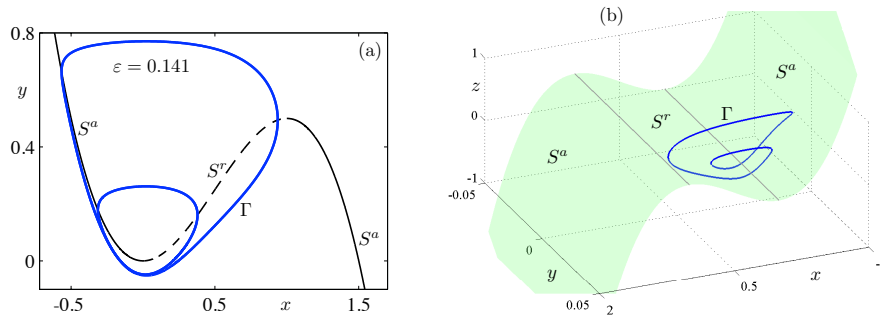


Figure 8. Mixed-mode periodic attractor of system (4.1) for $\varepsilon = 0.141$ and $f_2 = 1.5$, $f_3 = -1$, $g_1 = 0.2$. (a) shows a projection onto the (x, y) -space, where one can see that the mixed-mode oscillation Γ is formed by one small amplitude loop and one large amplitude loop, both enclosing convex areas of the plane. (b) shows a view of Γ in the (x, y, z) -space together with the critical manifold S_0 of the system.

a folded node. In the second case, mixed-mode oscillations have a more complicated pattern organised by canards at a folded saddle-node (for a description of folded nodes/saddle-nodes see Szmolyan & Wechselberger (2001)). It is natural to study the curvature of solutions in these scenarios to understand the difference between them. Here, however, we restrict attention to the dynamic canard explosion when $\mu + g_1$ is small.

(b) *Canard explosion and the inflection curve in the fast subsystem*

By reversing time, $t \mapsto -t$, we can write the fast subsystem of (4.1) in the same form as (3.6), that is, a singularly perturbed Liénard system with a constant forcing parameter

$$x' = y - f(x), \tag{4.2}$$

$$y' = \varepsilon(z - x), \tag{4.3}$$

where z is a parameter, and the prime denotes differentiation with respect to the fast time $\tau = -t/\varepsilon$. The function f is given by $f(x) = f_2x^2 + f_3x^3$, and therefore the critical manifold $y = f(x)$ has folds at $x = 0$ and $x = -2f_2/3f_3$. This implies that the repelling branch S^r of the critical manifold S_0 lies in the range $|3f_3x + f_2| < |f_2|$. Let us then apply the criterion (3.11) for the existence of an inflection curve in the fast subsystem, $|f'(x)| > 2\sqrt{\varepsilon}$. We find that an inflection point exists at x if

$$\text{either } f'(x) > +2\sqrt{\varepsilon} \iff |3f_3x + f_2|^2 < f_2^2 + 6f_3\sqrt{\varepsilon}, \tag{4.4a}$$

$$\text{or } f'(x) < -2\sqrt{\varepsilon} \iff |3f_3x + f_2|^2 > f_2^2 - 6f_3\sqrt{\varepsilon}, \tag{4.4b}$$

only the former of which is in the neighbourhood $|3f_3x + f_2| < |f_2|$ of S^r . It can be satisfied only if $f_2^2 + 6f_3 > 0$, hence if

$$\varepsilon < \varepsilon_0 := \left(\frac{f_2^2}{6f_3} \right)^2. \tag{4.5}$$

In figures 8-9 we use parameters $f_2 = 1.5$, $f_3 = -1$ and $g_1 = 0.2$, for which

$$\varepsilon_0 = \left(\frac{3}{2^3}\right)^2 = 0.140625. \quad (4.6)$$

We conclude that the z -dependent family of limit cycles of the fast subsystem contain canards (more specifically, non-convex canard cycles) only for $\varepsilon < \varepsilon_0$. It is easy to check by direct simulation that the mixed-mode periodic attractor of the full system does not have a change in the sign of its local curvature in the (x, y) -plane for $\varepsilon > \varepsilon_0$, see figure 8. Consequently, we propose that the slow passage through a canard explosion is well-defined only for $\varepsilon < \varepsilon_0$. Thus for any $\varepsilon < \varepsilon_0$, and for μ and g_1 chosen such that $\mu + g_1$ is $o(1)$, the system (4.1) possesses at least one mixed-mode periodic attractor of its fast subsystem, whose small amplitude [resp. large amplitude] oscillations resemble canards without head [resp. canards with head], and which undergoes a proper canard explosion upon variation of the slowest variable z considered as a parameter.

(c) *Canard-like behaviour in the full system*

The periodic attractor shown in figure 8 is not the only limit cycle of system (4.1). In fact, upon variation of μ , one can observe Hopf bifurcations occurring at $\mu = 0$ and $\mu = 0.1$, connected to one another by a one-parameter family of limit cycles. This bounds in μ the region of parameter space where single-mode oscillatory dynamics occurs. For the values of f_2 , f_3 and g_1 in figure 8, that region is $\mu \in [0, 0.1]$, in which range the dynamics of (4.1) is governed by a slow passage through a canard explosion.

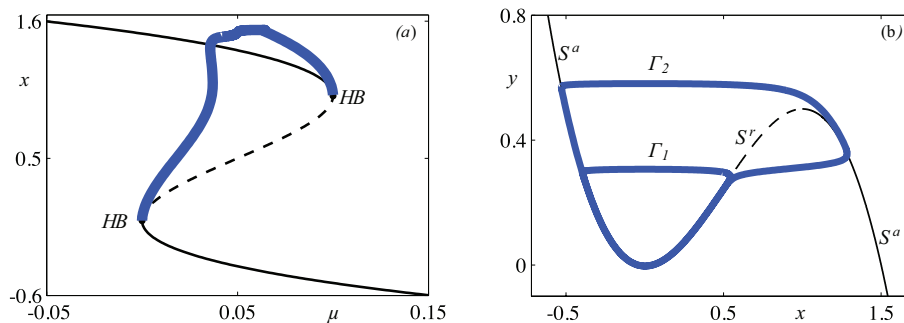


Figure 9. Bifurcations and canard-like cycles of the full system (4.1) obtained upon variation of the parameter μ , with $f_2 = 1.5$, $f_3 = -1$, $g_1 = 0.2$. (a) shows the bifurcation diagram with branches of equilibria (thin curve) and limit cycles (thick curve) born at Hopf bifurcation points (dots). (b) shows two limit cycles, Γ_1 for $\mu = 0.02$ and Γ_2 for $\mu = 0.036$ which share several aspects of canard cycles.

Look more closely at the bifurcation diagram presented in figure 9(a). As μ varies, the maximum value of the variable x along each cycle is plotted on the vertical axis. One observes that the branch of limit cycles connecting the two Hopf bifurcations has a sharp increase starting at the left Hopf point. The size of the μ -interval in which this sharp increase occurs, from small amplitude to large amplitude

limit cycles, is approximately 0.04. This is on the order of magnitude of the chosen value $\varepsilon = 0.01$, and lies outside the range of simple canard explosions (which take place within an interval of the control parameter that is exponentially small in ε). Despite this, in figure 9(b), one can clearly identify two characteristics of canard cycles that are present in these limit cycles of the full 3D system (4.1). First, both cycles remain close to the repelling sheet of the critical manifold S_0 for an $O(1)$ interval of time; second, the local curvature changes sign between the small and large limit cycles. Hence it seems reasonable to classify these as canard-like cycles. This was reported by Moehlis (2006) in the context of the Hodgkin-Huxley equations, where a two-dimensional subsystem displays a canard explosion, and the full four-dimensional system has a parameter-dependent family of limit cycles sharing some of the properties of canards, despite occurring in an interval of the control parameter that is *not* exponentially small in ε . They can be seen as canard-like (non-MMO) cycles, but they are much more robust than their two-dimensional relatives. This robustness is to be expected in systems with more than one slow variable, owing to the generic existence of robust canards described by Descroches & Jeffrey (2011).

To clarify the statement that such robust limit cycles are canard-like, we can apply the inflection criterion to place an upper bound on ε for canards to exist. For a general three time scale system of the form

$$x' = y - f(x), \quad (4.7a)$$

$$y' = \varepsilon g(x, y, z, \varepsilon), \quad (4.7b)$$

$$z' = \varepsilon^2 k(x, y, z, \varepsilon), \quad (4.7c)$$

whose fast subsystem (4.7a)-(4.7b) is a singularly perturbed Liénard system of the form (3.6), we follow the calculations detailed in section 3. Eliminating time, orbits must satisfy

$$\frac{dy}{dx} = \frac{\varepsilon g(x, y, z, \varepsilon)}{y - f(x)}, \quad (4.8)$$

$$\frac{dz}{dx} = \frac{\varepsilon^2 k(x, y, z, \varepsilon)}{y - f(x)}. \quad (4.9)$$

Considering these as curves parameterized by x , differentiating (4.8) with respect to x , and letting $y''(x) = 0$, we find the (two-dimensional) inflection surface given implicitly by (omitting arguments)

$$\frac{dg}{dx} h^2 + \left(\varepsilon^2 k \frac{dg}{dz} + \varepsilon g \frac{dg}{dy} + g \frac{df}{dx} \right) h - g^2 \varepsilon = 0, \quad (4.10)$$

where $h(x, y) = y - f(x)$. The criterion for the possible existence of canards becomes the condition that the quadratic equation (4.10) has a pair of real solutions $y = y_{\pm}(x, z)$, and that the inflection surface $(x, y_{\pm}(x, z), z)$ has branches in the neighbourhood of the repelling slow manifold S^r . For systems of the form we have considered, where f is a cubic function of x , S^r lies between the folds of the critical manifold $y = f(x)$, meaning that x must lie in the range $x \in (x_L, x_R)$ where $f'(x_L) = f'(x_R) = 0$. For (4.1), this predicts that a necessary condition for canards is

$$\varepsilon < \varepsilon_0 \approx 0.15.$$

This value is comparable to that obtained for the fast subsystem, which makes sense, since the full system behaves as a super-slow perturbation of its fast subsystem for the range of μ and g_1 considered. Note that the calculation above is based on considering only two components of curvature, corresponding to projections onto the (x, y) and (x, z) planes. A more general way of using curvature arguments in this context is provided in Ginoux & Rossetto (2006a,b), Ginoux (2009), where a method is developed to compute slow manifolds as loci of zero-curvature in planar systems, zero-torsion in three-dimensional systems, and more generally as loci of vanishing flow curvature in n -dimensional singularly perturbed dynamical systems. In particular, the inflection equations (3.4), (3.16) and (4.10) may be obtained by this method. These “flow curvature manifolds” have not been used with a focus on canards, but are closely linked to the more basic inflection curve criteria developed here.

5. Concluding remarks

In this paper, we made use of the inflection curve method as introduced in the chemical literature (Brøns 1988; Brøns & Bar-Eli 1994; Peng *et al.* 1991) to geometrically characterize the canard phenomenon. We found the dependence of the zero-curvature set on the time scale ratio ε . We showed that there exists a critical ε -value above which no inflection curve exists in the neighbourhood of the repelling sheet of the critical manifold. In particular, the distinction between convex small amplitude canards cycles without head, and non-convex large amplitude canard cycles with head, cannot be made for ε greater than the critical value ε_0 . This led to a convexity criterion for canards in planar singularly perturbed systems. The criterion does not establish that limit cycles exist, only that, if such cycles exist, then they can form canards. Finally, we extended this result to three time scale systems in \mathbb{R}^3 , where the inflection curve method gives an upper bound in ε , fixing the region where the so-called slow passage through a canard explosion is well defined.

The different tools applied to singularly perturbed systems here and in a related paper (Desroches & Jeffrey 2011), namely inflection curves, exponential microscopes, and pinching, all revolve around one idea which we believe is central to understanding of the canard phenomenon: extreme changes of local curvature. As described by Desroches & Jeffrey (2011), canards occur when transversality is lost between the vector field and certain zero-level sets associated with the flow. These level sets correspond to the second derivative of an exponential rescaling of the fast variable, and undergo a bifurcation when passing through the canard point, which is captured by the method of pinching. Similarly, the inflection criterion discussed here is based on the fact that the transition between small and large oscillations via the maximal canard coincides with the crossing of a zero-level set of the curvature of the flow. The more complex of the examples presented here have not yet been studied in detail using these ideas, the purpose of the current work being to illustrate how the method can refine the definition of a canard, and elucidate its role in the geometry of singularly perturbed systems. Work is ongoing to extend the more general ideas of Ginoux & Rossetto (2006a,b) and Ginoux (2009) to use flow curvature to find implicit equations for slow manifolds, to further study non-hyperbolic points and their role in the canard phenomenon.

References

- Benoît, E., Callot, J.-L., Diener, F. & Diener, M. 1981 Chasse au Canard. *Collect. Math.* **32**, 37–119.
- Brøns, M. 1988 Bifurcations and instabilities in the Greitzer model for compressor system surge. *Mathematical Engineering in Industry* **2**(1), 51–63.
- Brøns, M. & Bar-Eli, K. 1994 Asymptotic analysis of canards in the EOE equations and the role of the inflection curve. *Proc. R. Soc. Lond. A* **445**, 305–322.
- Bruce, J. W., & Giblin, P. J. 1992 *Curves and Singularities*, 2nd edn. Cambridge: Cambridge University Press.
- Diener, M. 1984 The canard unchained or how fast/slow dynamical systems bifurcate. *Math. Intelligencer* **6**(3), 38–49.
- Desroches, M., Guckenheimer, J., Krauskopf, B., Kuehn, C., Osinga, H. M. & Wechselberger, M. 2011 Mixed-mode oscillations in systems with multiple time scales. To appear in *SIAM Review* (in press).
- Desroches, M. & Jeffrey, M. R. 2011 Canards and curvature: nonsmooth approximation by pinching. Submitted to *Nonlinearity*.
- Fenichel, N. 1972 Persistence and smoothness of invariant manifolds for flows. *Indiana Univ. Math. J.* **21**, 193–226.
- Fenichel, N. 1979 Geometric singular perturbation theory for ordinary differential equations. *J. Differential Equations* **31**(1), 53–98.
- FitzHugh R. 1961 Impulses and physiological states in theoretical models of nerve membrane. *Biophys. J.* **1**, 445–466.
- Ginoux, J.-M. & Rossetto, B. 2006a Differential geometry and mechanics: Applications to chaotic dynamical systems. *Int. J. Bifur. Chaos* **16**(4), 887–910.
- Ginoux, J.-M. & Rossetto, B. 2006b Slow manifold of a neuronal bursting model. In *Emergent Properties in Natural and Artificial Dynamical Systems* (eds M. A. Aziz-Alaoui and C. Bertelle), pp. 119–128, New York: Springer-Verlag.
- Ginoux, J.-M. 2009 *Differential Geometry applied to Dynamical Systems*. World Scientific Series on Nonlinear Science, Series A, Vol. **66**, Singapore: World Scientific.
- Hindmarsh, J. L. & Cornelius, P. 2005 The development of the Hindmarsh-Rose model for bursting. In *Bursting: The Genesis of Rhythm in the Nervous System* (eds S. Coombes and P. C. Bressloff), pp. 3–18, Singapore: World Scientific.
- Hindmarsh, J. L. & Rose, R. M. 1984 A model of neuronal bursting using three coupled first-order differential equations. *Proc. R. Soc. Lond. B* **221**, 87–102.
- Hirsch, M. W., Pugh, C. C. & Shub, M. 1977 *Invariant manifolds*. Lecture Notes in Mathematics Vol. **583**, Berlin: Springer-Verlag.
- Krupa, M., Popović, N. & Kopell, N. 2008 Mixed-Mode Oscillations in Three Time-Scale Systems: A Prototypical Example. *SIAM J. Appl. Dyn. Syst.* **7**(2), 361–402.
- Krupa, M. & Szmolyan, P. 2001 Relaxation oscillation and canard explosion. *J. Diff. Eq.* **174**(2), 312–368.
- Kuznetsov, Y. A. 2004 *Elements of Applied Bifurcation Theory*, New York: Springer-Verlag.
- Moehlis, J. 2006 Canards for a reduction of the Hodgkin-Huxley equations. *J. Math. Biol.* **52**, 141–153.
- Peng, B., Gaspar, V. & Showalter, K. 1991 False bifurcations in chemical systems: canards. *Phil. Trans. Phys. Sci. Engr.* **337**(1646), 275–289.
- Popović, N. 2008 Mixed-mode dynamics and the canard phenomenon: Towards a classification. *J. Phys.: Conf. Ser.* **138**, 012020.
- Szmolyan, P. & Wechselberger, M. 2001 Canards in R^3 . *J. Differ. Equ.* **177**, 419–453.
- Van der Pol, B. 1926 On “relaxation oscillations”. *Phil. Mag. Ser. 7* **2**(11), 978–992.

Wechselberger, M. 2005 Existence and bifurcation of canards in \mathbb{R}^3 in the case of a folded node. *SIAM J. Appl. Dyn. Syst.* **4**(1), 101–139.